Sensing and Bio-Sensing Research 47 (2025) 100755

Contents lists available at ScienceDirect

Sensing and Bio-Sensing Research

journal homepage: www.elsevier.com/locate/sbsr

A CRISPR/Cas12a electrochemical biosensing to detect pig mtDNA D-loop for ensuring food authenticity

Muhammad Ihda H.L. Zein [a,b], Clianta Yudin Kharismasari [a], Ari Hardianto [a], Salma Nur Zakiyyah [a], Riezki Amalia [c], Mehmet Ozsoz [a,d], Mara Mirasoli [b], Irkham [a,*], Yeni Wahyuni Hartati [a,*]

[a] Department of Chemistry, Faculty of Mathematics and Natural Sciences, Universitas Padjadjaran, Bandung 45363, Indonesia
[b] Department of Chemistry "Giacomo Ciamician", Alma Mater Studiorum - University of Bologna, Bologna 40126, Italy
[c] Department of Pharmacology and Clinical Pharmacy, Universitas Padjadjaran, Bandung 45363, Indonesia
[d] Department of Biomedical Engineering, Near East University, Mersin 99138, Turkey

ARTICLE INFO

Keywords:
CRISPR/Cas12a
Electrochemical biosensor
Food monitoring
Optimization
BBD (box-Benhken design)

ABSTRACT

Ensuring safe and accurately labeled food products is crucial for communities worldwide. One significant concern in food safety is the unintended inclusion of pork in products, which impacts food labeling, religious dietary practices, legal standards, and public health. Detecting such contamination is challenging due to complex food processing, requiring advanced methods for accurate identification. A CRISPR/Cas12a-based electrochemical biosensor has garnered attention for its rapidity, portability, high sensitivity, and specificity, leveraging trans-cleavage activity for precise detection. This study utilized a modified electrode, SPCE/Ceria/STV/Biotin-ssDNA-Methylene Blue (MB), characterized by SEM/EDX and voltammetry methods to examine morphology and electrochemical behavior. Optimization using the Box-Behnken Design (BBD) yielded ideal conditions: 30 min STV incubation, 1.5 μM probe concentration, 240 min probe incubation, 0.1 % BSA concentration, 30 min target incubation, and 2 μL target volume. These parameters enabled the development of an ultrasensitive biosensor with detection and quantification limits of 4 fM and 71 fM, respectively. Operating within a range of 10 nM to 100 fM, the biosensor achieved 1.1 % RSD. This CRISPR-based biosensor successfully detected pig mtDNA in raw and processed meat samples, achieving a 100.82 % recovery rate for corned samples and maintaining stability for 14 days. These findings highlight the biosensor's potential as a rapid, stable, ultrasensitive, and ultraspecific alternative for food monitoring. Its robustness makes it particularly suitable for ensuring the authenticity of animal-derived food products susceptible to counterfeiting.

1. Introduction

The authenticity of meat products is a pressing issue for consumers and regulatory bodies. Economic motives drive some manufacturers to replace premium meats with cheaper alternatives, often without declaring on labels. The case of pork is particularly concerning because the meat can be substituted in products intended for consumers with allergies and for Muslim or Jewish communities that avoid this meal for religious reasons. Despite legislation requiring clear labeling of raw materials, adulteration of meat products with pork remains a concern, as thermal treatments complicate species identification in processed food. Detecting mitochondrial DNA (mtDNA) offers a powerful solution because the high copy number and resilience to processing conditions allow for greater sensitivity and reliability in identifying even trace pork contamination. Therefore, this study examines the importance of mtDNA detection as an essential tool to address health, ethical, and regulatory challenges in meat authentication.

DNA-based detection has advantages over protein or fat-based methods, such as greater resistance to degradation, increased specificity, and sensitivity [1]. Some advanced nucleic acid-based detection methods include RT-Evagreen PCR [2], species-specific PCR [3], PCR-RFLP [4], PCR-Taqman [5], and RT-PCR or qPCR [6]. In these methods, mtDNA was often used as a target biomarker for pigs because the *cytochrome b* gene (*CYTB*) and *D-Loop* region of mtDNA were highly variable, allowing differentiation between species, including pigs [1,7]. However, the PCR method has limitations, such as long analysis times,

* Corresponding authors.
E-mail addresses: irkham@unpad.ac.id (Irkham), yeni.w.hartati@unpad.ac.id (Y.W. Hartati).

https://doi.org/10.1016/j.sbsr.2025.100755
Received 19 December 2024; Received in revised form 22 January 2025; Accepted 28 January 2025
Available online 1 February 2025

expensive equipment and reagents, and the need for skilled operation [8]. Electrochemical biosensor offers a promising alternative to traditional PCR methods for detecting pork mtDNA, because the equipment provides rapid, cost-effective, and user-friendly solutions with high specificity and sensitivity, eliminating the need for extensive laboratory equipment and skilled personnel. By integrating advanced detection methods, this biosensor can significantly streamline the identification of species in food products while reducing analysis times and operational complexities.

In recent times, CRISPR-Cas electrochemical biosensor gained attention due to the ability to detect nucleic acid with ultra-high sensitivity and selectivity, often without the need for an amplification method. This system integrates Clustered Regularly Interspaced Short Palindromic Repeats (CRISPR) with CRISPR-associated (Cas) proteins to provide adaptive immunity against foreign elements in bacteria and archaea [9–11]. The CRISPR/Cas12 system is particularly useful for developing specific dsDNA or ssDNA as a target. Previous studies have developed highly sensitive and rapid detection methods for viruses, such as SARS-CoV-2 using CRISPR-Cas12-based assays, showing the potential as an in situ diagnostic tool [12]. The system was used in the authentication of halal food and the detection of pathogenic microorganisms, showing the versatility in various applications [13]. Additionally, CRISPR-Cas12 was integrated into biosensor for diagnostics, facilitating the specific and sensitive detection of diverse targets [14]. Advancements in CRISPR-Cas12 technology have resulted in the creation of rapid and specific detection modules for viruses, such as SARS-CoV-2, combining robust virus amplification with precise detection capabilities [15]. Furthermore, CRISPR-Cas12 played a significant role in identifying COVID−19 variants by detecting single nucleotide polymorphism mutations in the SARS-CoV-2 spike gene [16]. The system was also applied to monitor bacteria at the species level in fermentation processes, showing the utility across various fields [17]. Wu et al. (2021) showed the success of this method for detecting pig DNA using fluorescence. CRISPR/Cas12a was shown to increase specificity due to cis-cleavage and trans-cleavage activity [13].

The simplicity of electrochemical biosensor is shown by the use of screen-printed carbon electrodes (SPCEs), which offer a compact design featuring all three electrodes integrated into a single, small module. Furthermore, the disposable nature makes SPCE ideal for single-use biosensor strips for rapid and quantitative detection [63]. These electrodes can be modified with different materials, such as carbon nanotubes, graphene, or metal nanoparticles, to enhance electrochemical properties and sensitivity [18,19]. SPCE can also be modified with conductive materials, such as CeO_2 (ceria), to enhance sensitivity and biocompatibility for DNA detection. The use of Ceria modification in SPCE can increase the electroactive surface area and electron transfer rate between the electrode and the analyte [20]. Ceria also creates shorter steps than AuNPs to modify SPCE with a streptavidin (STV)-biotin system [21]. The SPCE/CeO_2 has also been reported for detecting pig DNA with free-label electrochemical biosensor. This component has a detection, limit, and precision of 0.0303 μg/mL, 4.81 μg/mL, and 98.99 %, respectively [22].

Optimization of key parameters influencing response current is essential for achieving high sensitivity in detection methodologies. The Box-Behnken Design (BBD) is a statistical experimental design commonly used in response surface methodology (RSM) for optimizing processes. This method examines the effect of multiple variables or parameters on a response of interest. BBD is a second-order design that does not include a full factorial or fractional factorial design. This design is characterized by a three-level factorial for three or more factors, with points selected from a system arrangement [23]. Furthermore, designs combine two-level factorial with incomplete block design in a special manner, ensuring efficiency for optimization studies. BBD also enables studies to examine the interactions between variables efficiently with a relatively small number of experimental runs compared to full factorial design.

In this study, CeO_2 was electrodeposited on SPCE using a cyclic voltammetry (CV) method. The SPCE/CeO_2 was immobilized with STV and a biotin-ssDNA-MB probe through specific binding between STV and biotin [20]. A complex was formed between CRISPR/Cas12a, gRNA, and the target. From a previous study, an in-silico study was conducted to determine the gRNA sequence that could specifically and sensitively hybridize with the pig mtDNA *D-Loop* target with an Off-target value of 99.8 [24]. CRISPR/Cas12a recognizes the target via the PAM sequence, performing cis-cleavage on pig ssDNA and trans-cleavage on the ssDNA-MB probe on the electrode. A high and low MB signal shows the absence and presence of pigs, respectively. To achieve optimal detection, parameters were selected from a literature review [13,25,26] and optimized using the Box-Behnken experimental design. Finally, the performance of the resulting method is presented, including LOD, LOQ, RSD, stability, specificity, and %recovery in real samples.

2. Materials and methods

2.1. Chemicals and materials

The materials used in this study were demineralized water (PT Ikapharmindo Putramas, Indonesia), nuclease-free water (Promega, USA), biotinylated ssDNA probe-MB (biotin 5′- GGG TTT TTT GGG-3′ metilen blue) (Bioneer, Korea), CRISPR Cas12a (GenScript, USA), gRNA (5′- UAA UUU CUA CUC UUG UAG AU GAU UGU CGU GCC GGA UCA UGA GUU -3′) (Greiner Bio-One, Japan), Target mtDNA (5′- CAT GGA ACT CAT GAT CCG GCA CGA CAA TCC AAA CAA GG −3′) (Greiner Bio-One, Japan), cerium (III) nitrate hexahydrate ($Ce(NO_3)_3.6H_2O$) (Merck, Germany), potassium ferricyanide ($K_4[Fe(CN)_6]$) (Merck, Germany), potassium chloride (KCl) (Merck, Germany), phosphate-buffered saline (PBS) and pH 7.4 (Merck, Germany). Other materials include bovine serum albumin (BSA) (Merck, Germany), STV (Promega, USA), magnesium chloride hexahydrate ($MgCl_2.6H_2O$) (Merck, Germany), natrium chloride (NaCl) (Merck, Germany), Tris-Base (Merck, Germany), and Kit Meat Extraction.

2.2. Instrumentations

The SPCE (Metrohm DropSens, Switzerland) was used as a carbon for working and auxiliary, and Ag as a reference electrode for the electrochemical transducer. The electrochemistry measurements were conducted using a Zimmer & Peacock potentiostat connected to a computer using PSTrace 5.9 software (Zeamer & Peacock, UK). A scanning electron microscope (SEM) (Hitachi TM3000, Japan) was used for electrode surface morphology analysis. Other instruments used include a pH Meter (Mettler Toledo, USA), mini dry bath (JOANLAB, China), mini centrifuge MCF-1350 (DIVERS DUTSCHER, Netherlands), and vortex (IKA, Germany).

2.3. Fabrication of the electrochemical biosensor

The SPCE surface was rinsed with demineralized water and dried at room temperature. Afterward, 40 μL of cerium nitrate solution 1000 ppm was electrodeposition onto the surface of the SPCE and then run CV over a range of −0.1 to 1.0 V at a scan rate 0.1 V/s, E_{step} 0.02 V, and number of scans of 15. The SPCE/CeO_2 was rinsed with demineralized water and dried at room temperature before being electrochemically characterized by differential pulse voltammetry over a potential range − 0.3 to 0.5 V at a scan rate 0.008 V/s, E_{step} 0.004 with an E_{pulse} 0.025 V, and pulse of 0.05 s. SPCE was also characterized before and after modification using SEM.

The SPCE/CeO_2 was incubated with STV solution for 30 min at 4 °C. Subsequently, SPCE/CeO_2/STV were rinsed with PBS solution pH 7.4 0.01 M. Biotinylated ssDNA probe-MB were incubated for 4 h at 37 °C in dry incubator, then rinsed with Tris-HCl pH 7.4 0.01 M. After the probe was successfully immobilized on the surface of the SPCE/CeO_2 electrode

with the STV-biotin system, the non-specific binding site on the electrode surface was incubated using 0.1 % BSA solution for 10 min at 25 °C, and then rinsed with PBS solution pH 7.4 0.01 M.

2.4. Pig mtDNA D-loop detection with CRISPR/Cas12 system

A total of 10 µL of 100 nM Cas 12a and 10 uL of 100 nM gRNA were added, vortexed for 5 min, then centrifuged for 5 min at 1500 rpm. Duplex Cas12a/gRNA was added with varying target concentrations, vortexed for 5 min, then centrifuged for 5 min at 1500 rpm. Furthermore, a triplex was added to the electrode and incubated for 30 min at 37 °C in the dry incubator. SPCE was rinsed with 40 µL Tris-HCl 0.01 M solution pH 7.4 and allowed to dry, then measured by square wave voltammetry over a potential range − 0.6 to 0.0 V at an E_{step} 0.004 V, amplitude 0.025 V with a frequency 25 Hz using 0.1 M PBS + 0.1 M KCl electrolyte.

2.5. Determination of optimum conditions from parameters affecting experiments

Factors, such as STV incubation time, probe DNA concentration, incubation time of probe DNA, BSA concentration, pig mtDNA incubation time, and volume of pig mtDNA were selected to be optimized in the experiment. Each factor was designed at three different levels, namely lowest (−1), medium (0), and highest (+1), as shown in Table 1. The response of the measurement results from the experiment was then processed and the optimum value of each of these factors was determined using the Box-Behnken experimental design with *Jupyter Notebook* software.

2.6. Sample preparation and DNA extraction

Fresh samples of pork, beef, mutton, chicken, duck, and rabbit, as well as commercially corned pork and corned beef, were purchased from local markets. Samples were stored at −20 °C until needed for analysis. For each sample, 25–50 mg of meat was cut into pieces and ground with pestle and mortar into powder in a pestle and mortar using liquid nitrogen. Genomic DNA from all types of meat was extracted using a DNA Isolation Kit according to the instructions. Animal tissue was added to Buffer Digestion to lyse all cells, then Buffer PA, isopropanol, and 75 % ethanol were sequentially added to extract DNA. Finally, the remaining ethanol was evaporated and the DNA was dissolved in 50 µL H_2O. Extracted DNA was either immediately used for subsequent experiments or stored at −20 °C.

3. Results and discussion

3.1. Fabrication and characterization of the electrode

Fig. 1a shows the step-by-step modification of the electrode. The ceria electrodeposition reaction process on the SPCE surface was carried out with CV method [27]. The oxidation reaction of Ce^{3+} to Ce^{4+} occurs with the following stages:

Table 1
Optimization factors affecting the experimental conditions.

No.	Parameter	Level		
		-1	0	+1
1.	STV incubation time	10 min	30 min	50 min
2.	probe DNA concentration	0,5 µM	1 µM	1,5 uM
3.	probe DNA incubation time	120 min	180 min	240 min
4.	BSA concentration	1 %	0.1 %	0.01 %
5.	pig mtDNA incubation time	30 min	60 min	90 min
6.	pig mtDNA Volume	2 uL	5 uL	10 uL

$$Ce(OH)_2{}^{2+} \rightarrow CeO_2 + 2\,H_2O \quad (1)$$

A $K_4[Fe(CN)_6]$ solution was used as a mediator to test the electrode changes before and after the modification process. The reduction and oxidation reactions that occur in $K_4[Fe(CN)_6]$ are shown in Eqs. (2), (3) [28].

$$\left[Fe(CN)_6\right]^{3-} + e \rightleftharpoons \left[Fe(CN)_6\right]^{4-} \quad (2)$$

Methylene Blue (MB) was used as a signal tag on ssDNA for final results of trans-cleavage activity from CRISPR/Cas12a, due to excellent redox properties [29]. During a reduction reaction at the cathode, MB was reduced to Leucomethylene Blue (LMB)

$$MB + 2H^+ + 2e^- \rightleftharpoons LMB \quad (3)$$

Fig. 1b shows the DPV results for the modification of an SPCE with ceria (red line). The figure shows that the oxidation peak currents of $K_4[Fe(CN)_6]$ using SPCE/ceria are increased generally compared to a bare electrode (black line). Furthermore, the modification using ceria was found to increase the current 1.64 times. This is due to an increase in the conductivity of ceria in the electrode by increasing electron transfer between the electrode and analyte, compared to bare SPCE. Meanwhile, ceria was observed using the SEM image shown by the difference with bare SPCE (SI). This result shows that ceria was successfully incorporated onto the surface of the electrode through electrodeposition. The SPCE modified with ceria was further immobilized with STV (blue line). DPV characterization showed decreased peak current due to inhibition of electron transfer on the surface of the electrode. A higher resistance of the electrode was also observed due to large biomolecule immobilization, showing a successful immobilization. Meanwhile, the peak shifted slightly upon surface modification. The observed phenomenon may arise due to the intercalation of biomolecules during electron transfer, causing a shift in the potential. Current peaks targeting biomolecules, such as proteins, may experience conformational alterations during interaction with electrodes or signal molecules. These variations can influence the electron-transfer dynamics and consequently result in shifts in the current signal. Fig. 1c shows the SWV results for the modification of an SPCE/ceria/STV/ssDNA-MB (blue line). Similarly, the oxidation peak currents of MB follow a similar concept to those of $K_4[Fe(CN)_6]$ but differ in the potential of the oxidation peak. There was an increase in the peak currents using SPCE/ceria/STV/ssDNA-MB compared to a bare electrode without MB (red line).

Ceria facilitates the binding of STV to the electrode through strong interaction with $-NH_2$ groups, binding to both STV and thionine. Additionally, nanoceria reportedly forms bridge bonds with the carboxyl functional groups of antibodies without the need for additional agents [20]. The STV biomolecule on the electrode surface can specifically bind to the ssDNA-MB, which has a biotin end. The STV − biotin interaction is one of the strongest noncovalent interactions in nature due to high affinity [20]. These interactions include hydrogen bonds and van der Waals forces, which are hydrophobic. The STV − biotin binding is also similar to the antibody-antigen interaction, functioning as a lock and key, and occurs through a noncovalent interaction between a protein and a ligand [20]. Furthermore, ssDNA-MB immobilization leads to an interaction between STV, biotin, and the ssDNA-MB. The SPCE/Ceria/STV/ssDNA-MB complex was incubated with a 0.1 % BSA solution to cover the unmodified active sites on the SPCE surface. This process prevents any current measurements that could interfere with the analytical results of the analytes. The successful electrode modification process was strengthened by characterization using SEM-EDX, as shown in Fig. S1.

3.2. Optimization parameter with BBD

The electrode fabrication condition was optimized using a BBD before applying for the detection of the pig mtDNA D-loop target.

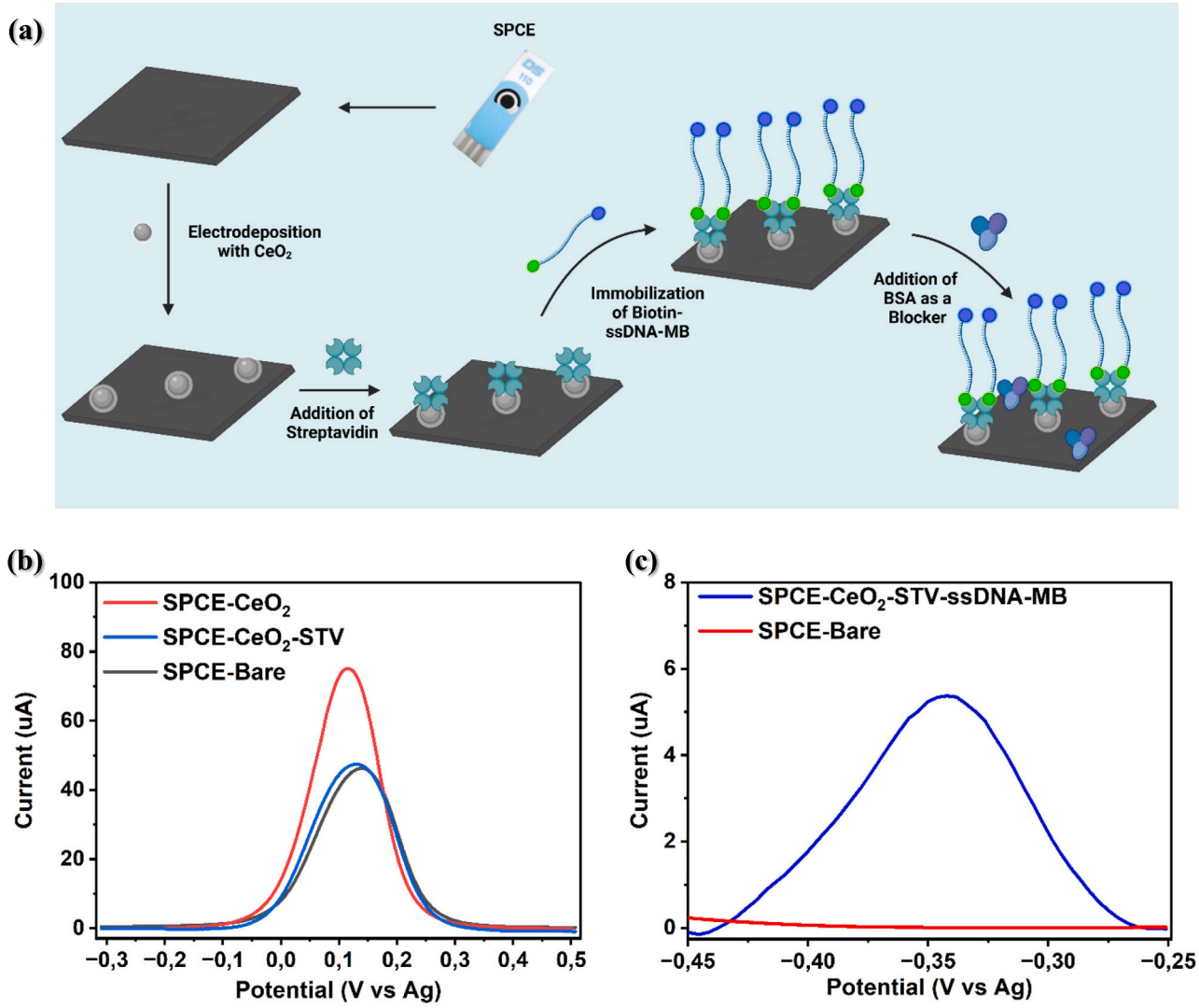

Fig. 1. (a) Step-by-step modification of SPCE and voltammetric characterization result of (b) DPV of bare SPCE, SPCE/ceria, SPCE/ceria-/STV using a redox system of $K_4[Fe(CN)_6]$ in 0.1 M KCl solution (c). SWV of SPCE bare, SPCE/Ceria/STV/ssDNA-MB using MB redox system.

Several parameters including STV incubation time, probe concentration, probe incubation time, BSA concentration, target incubation time, and target volume were optimized, as shown in Tables S1 and S2. BBD consists of 12 experimental sequences from the three levels of parameters, combined with various other parameters to form a cube-like area, and 3 center points. This serves as an index of the homogeneity of an experimental sequence. The center points are often placed at the beginning, middle, and end of the experimental design. Furthermore, the optimum conditions were determined using various voltammograms shown in Fig. S2 and are listed in Table S3. The equation explains the effect of the between the three levels of a parameter on a response, either positively or negatively.

Based on Fig. 2a and the coefficient of the response function, the incubation time of STV increased the current generated up to 30 min, after which further increases in time did not result in significant changes. This was related to the amount of STV immobilized on the electrode surface, which then binds to the biotinylated ssDNA-MB. Additionally, higher probe concentrations and longer incubation times lead to greater current generation. This phenomenon also suggests a higher number of probes attached to the electrode. However, considering the value of the current increase, the concentration and incubation time were set at 1 μM and 240 min, respectively (Fig. 2b and c). Some contours are saddle-shaped, showing that the experiment results are not yet optimal. Lower BSA concentrations also reduce the current, which is related to the smaller number of BSA molecules compared to ssDNA-MB, enabling CRISPR to perform optimally during target cutting (Fig. 2d). Conversely, using a high concentration of BSA produces an irregular current and can interfere with CRISPR performance during target cutting, leading to higher current. This is due to the size and number of BSA molecules compared to ssDNA-MB (Fig. 2e). Faster target incubation times correlate with reduced current output, a phenomenon attributed to the accelerated target-cutting process, thereby rendering additional time unnecessary. The target volume relates to the ratio between the triplex—CRISPR/Cas12a, gRNA, and the target, where the duplex concentration between CRISPR/Cas12a and gRNA is at a 1:1 ratio. In this case, the target concentration needs to be lower to avoid interfering with duplex formation and ensure CRISPR can function optimally, as shown in Fig. 2f.

3.3. *Target detection using CRISPR/Cas12a system*

The voltammogram was recorded using the MB redox system in a PBS electrolyte with 0.1 M KCl, within a potential range of −0.4 to 0.2 V. The results show that the peak current drops by approximately 70 % in the presence of the target, suggesting the activation of CRISPR/Cas12a. This differential cleavage of ssDNA-MB in active and inactive states

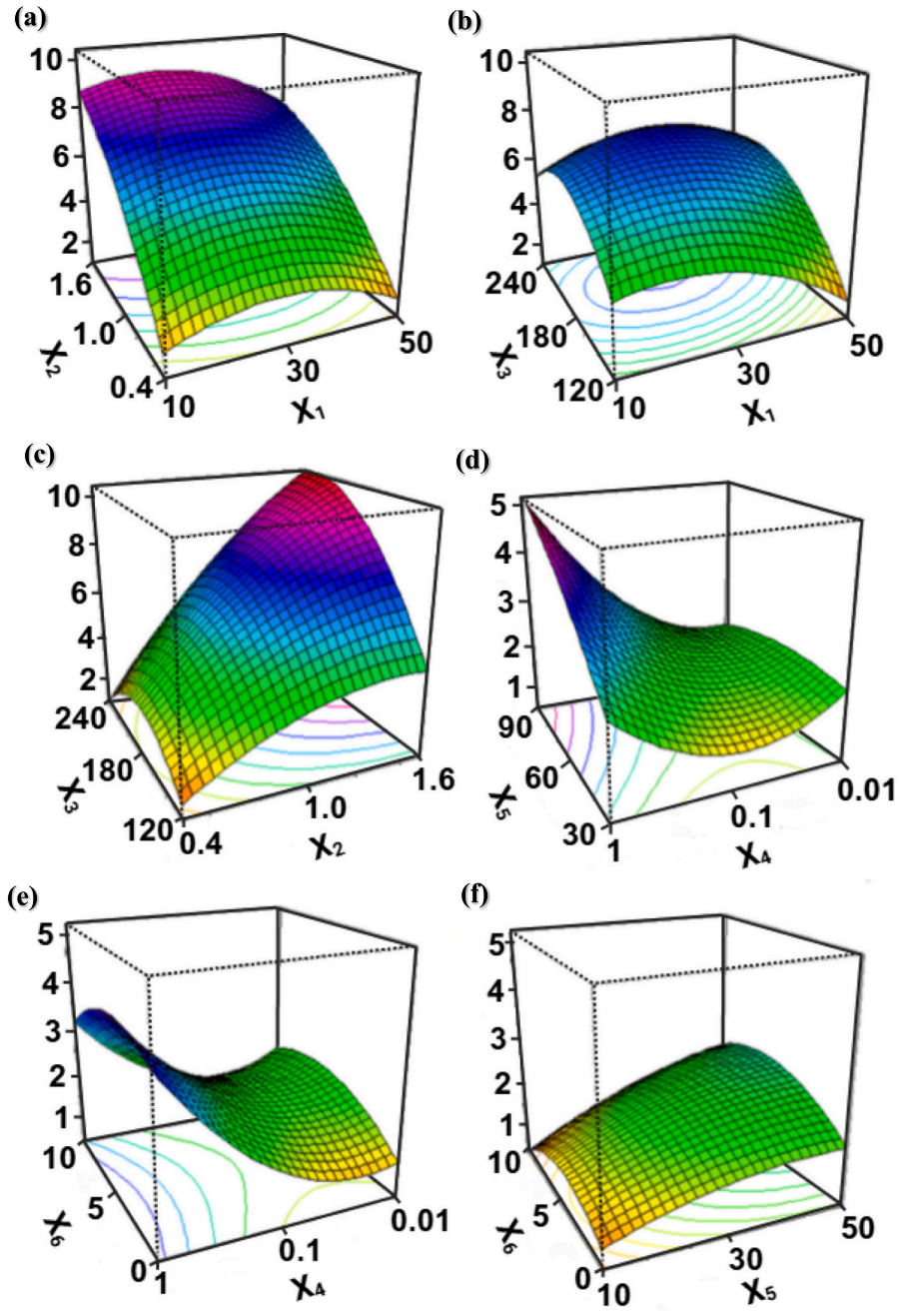

Fig. 2. Contour Plot of BBD for (a, b, c) parameters of SPCE-Ceria-STV-ssDNA-MB optimization; (d, e, f) parameters of target detection with CRISPR/Cas12a. X_1: STV incubation time (min), X_2: probe DNA concentration (μM), X_3: probe DNA incubation time (min), X_4: BSA concentration (%), X_5: pig mtDNA incubation time (min), X_6: pig mtDNA Volume (μL).

affects the peak current, as shown in Fig. 3a. The optimized voltammogram results are shown in Fig. 3b. Calibration curves were generated by varying the concentration of the pig mtDNA target, then the detection limit and quantification of the CRISPR/Cas12a-based biosensor were calculated. This experiment followed the procedure for determining the target response with CRISPR/Cas12a, using optimized parameters. Various concentrations of pig mtDNA target, namely 10 nM, 1 nM, 100 pM, 10 pM, 1 pM, and 100 fM were tested on the CRISPR/Cas12a-based biosensor, with each concentration measured three times. The resulting electrochemical response was measured using SWV, as shown in Fig. 3c.

Peaks were observed for concentration variations ranging from 10 nM to 100 fM, which were then adjusted by subtracting the control signal to obtain the ΔI value. This was plotted on the linear regression in Fig. 4a, with a correlation coefficient (R^2) of 0.9941. The limit of detection (LOD) was determined to be approximately 4 fM, and the limit of quantification (LOQ) was 71 fM. The precision test was conducted using seven measured electrodes resulting in an RSD value of 1.1 %, as shown in Fig. 4b. Based on these precision results, the repeatability of this method was concluded to be excellent.

Fig. 5a shows the results of the stability measurement and the test was carried out with optimized parameters by another study [30]. This optimization includes using silica gel with air and light-tight conditions at 4 °C. On the measured electrode, there was a decrease on days 7 and 14 but still within 5–10 %, and a drastic decrease on day 28. Therefore, the electrode was concluded to be stable at 14 days. Figs. 5b and 6a are the results of selectivity measurements on various species of raw meat

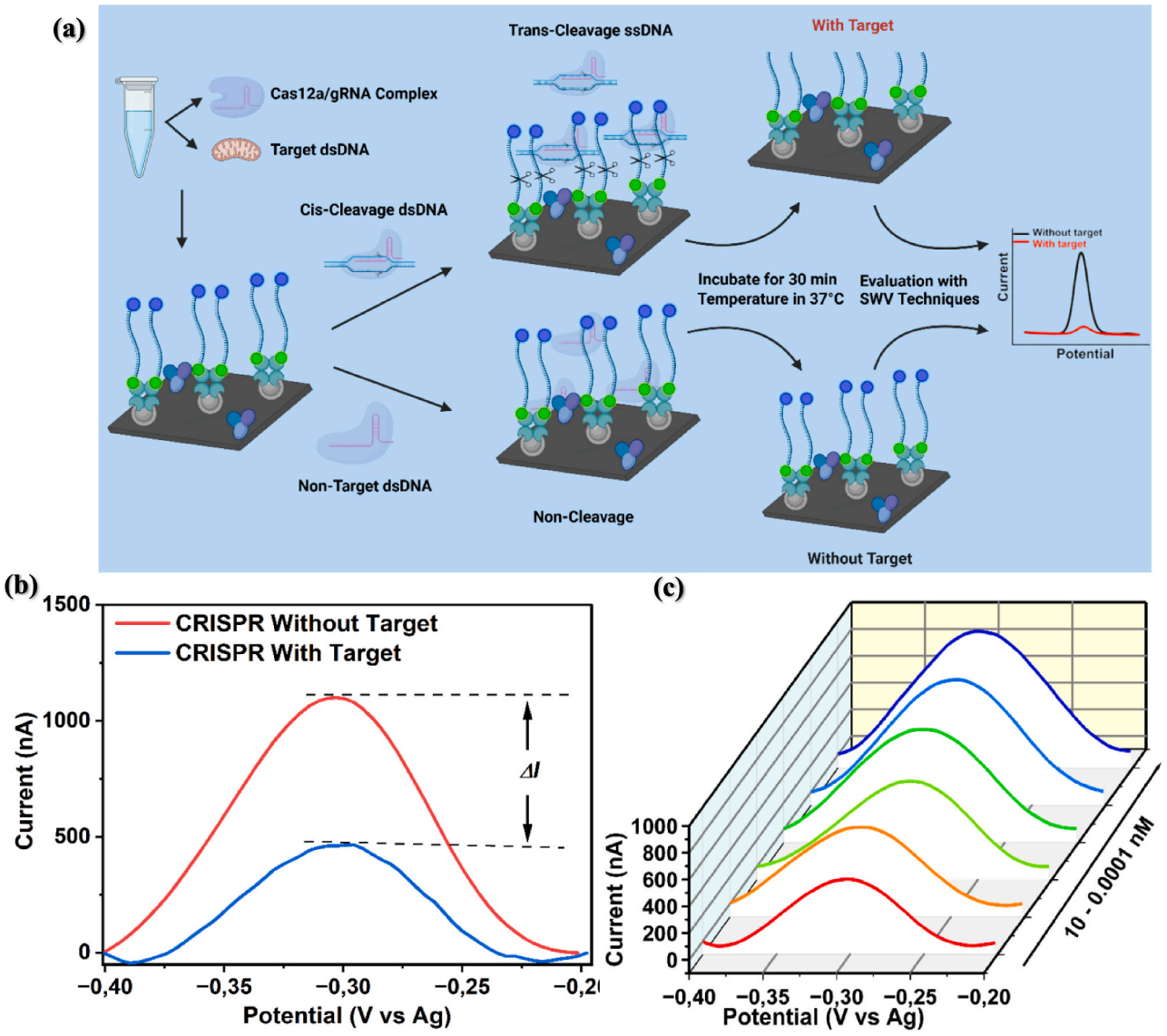

Fig. 3. Target detection with CRISPR/Cas12a: (a) Mechanism of on-off target detection mediated by MB signal using the main and trans-cleavage activities of CRISPR/Cas12a; (b) SWV voltammogram of target detection utilizing the Methylene Blue (MB) redox system with PBS electrolyte in 0.1 M KCl; (c) SWV voltammogram of target detection with various target concentrations. (For interpretation of the references to colour in this figure legend, the reader is referred to the web version of this article.)

samples and mixtures. Selectivity tests were carried out on animal species that were considered to be a mixture of pork. Selectivity values for different raw meat samples were 91.87 %, while for mixed samples, the lowest detection was carried out up to 0.1 %. This result shows good selectivity against a mixture of beef and pork. This is due to the use of gRNA and CRISPR, which are highly selective to the target DNA sequences, ensuring that the cutting of ssDNA probes will not occur. In Fig. 6b, real sample analysis was carried out on processed meat samples, namely corned beef. The result showed a significant difference between corned beef and pork, suggesting good selectivity for processed food detection and the percent recovery value for the real sample was 100.86 %. All voltammograms that correspond with these results are presented in Fig. S3, and the comparison between this work with other biosensor for food adulteration is shown in Table 2.

4. Conclusion

In conclusion, ultrasensitive detection of Pig mtDNA *D-loop* with CRISPR/Cas12a-based electrochemical biosensor has been successfully used to detect food adulteration in both raw and processed food samples. The use of CRISPR/Cas12a enabled more selective and sensitive measurements. The modified SPCE using ceria showed a 1.64 time increase in current compared to the bare SPCE, with characterization performed using the voltammetric method and SEM/EDX. The fabricated biosensor could detect pig mtDNA *D-loop*, shown by changes in electrochemical signals. This detection resulted from the main cleavage of the mtDNA target. This process triggered the trans-cleavage of MB between the mtDNA target and non-target. The optimized electrochemical biosensor based on CRISPR/Cas12a showed precision with an RSD value of 1.1 %, with a limit of detection (LOD) of 4 fM and a 71 fM limit of quantification (LOQ). Selectivity values for different raw meat samples were 91.87 %, while for mixed samples, the lowest detection level was 0.1 % w/w, with a recovery rate of 100.81 % for corned samples. The biosensor remained stable for up to 14 days. This result showed that CRISPR/Cas12a can enhance the sensitivity and specificity of biosensor, holding promise for developing a rapid, ultrasensitive, and portable method for the detection of food adulteration.

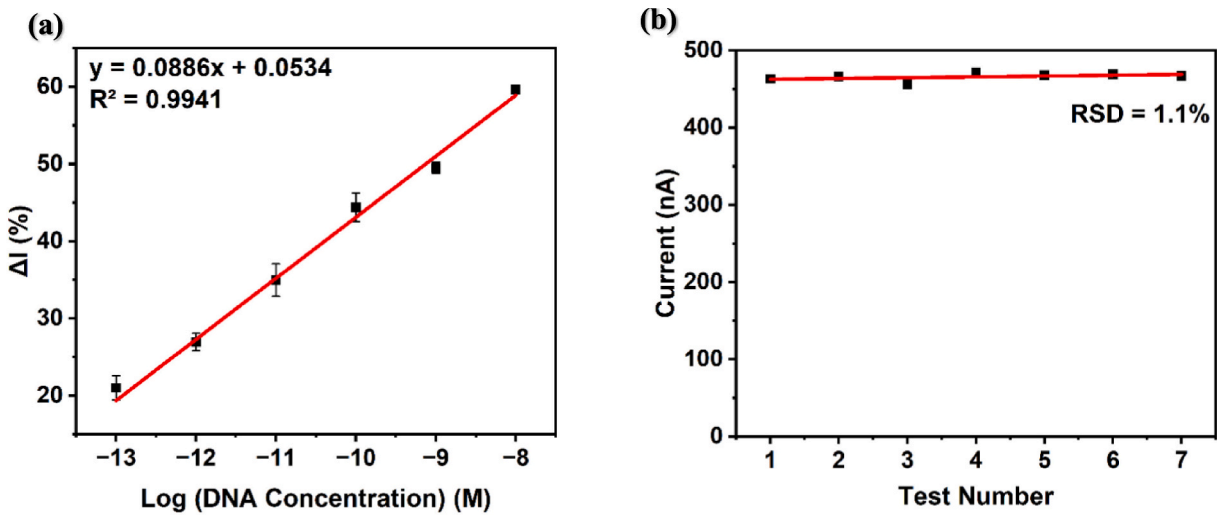

Fig. 4. (a) Calibration curve of the CRISPR/Cas12a-based biosensor with varying concentrations of pig mtDNA target; (b) SWV measurement results for precision testing at a 100 nM pig mtDNA target concentration.

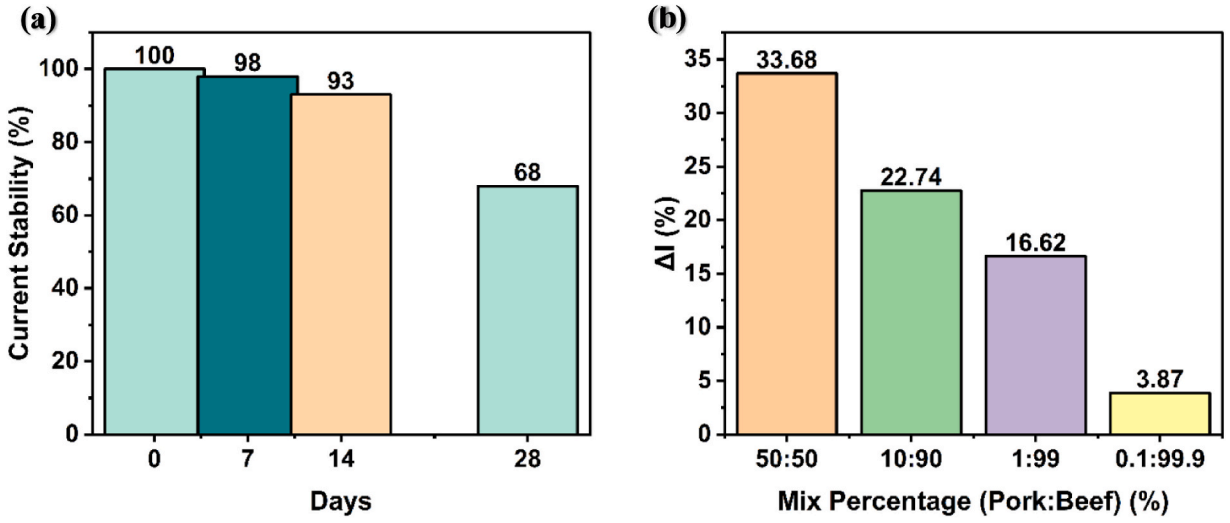

Fig. 5. Results for (a) the stability test with a period of 7, 14, and 28 days using the MB redox system with PBS electrolyte in 0.1 M KCl. Selectivity of (b) mix percentage between beef and pork.

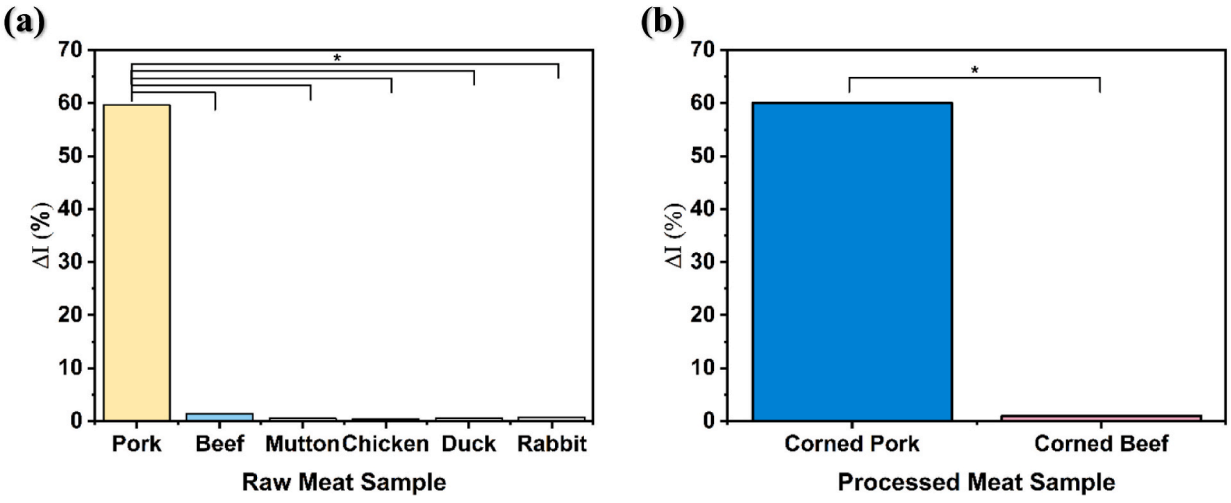

Fig. 6. Selectivity of (a) raw meat sample; (b) processed meat sample.

Table 2
Comparison of the performance of the developed biosensor for pig detection.

Method (target)	LOD	Linear range	Reference
Fluoresence Immunosensor based on magnetic bioseparation (pig IgG antibodies)	0.031 μg/L	0.75–23.50 μg/L	[31]
Surface plasmon resonance Immunosensor functionalized cGO-Au nanostars (pig IgG antibodies)	0.0375 μg/mL	0.0375–40 μg/mL	[32]
label free electrochemical immunosensor using SPCE (porcine serum albumin)	0.5 pg/mL	0.5–500 pg/mL	[33]
Label free and regentless Genosensor using SPCE modified with graphene acid (Pig mtDNA *CYTB*)	9 % *w*/w (pork/beef)	–	[34]
Optimized Label-Free Electrochemical Genosensor using SPCE/Au (Pig mtDNA *CYTB*)	0.135 μg/mL 5 % w/w (pork/beef)	0.5–1.5 μg/mL	[1]
Electrochemical Genosensor using SPCE/cerium (Pig mtDNA *CYTB*)	0.0303 μg/mL	5.0–30.0 μg/mL	[22]
Fluoresence Genosensor based on CRISPR-Cas12 (Pig mtDNA *CYTB*)	2.7 ng/μL	1–10 ng/μL	[13]
Optimized Electrochemical Biosensor based on CRISPR-Cas12a using SPCE/ceria (Pig mtDNA *D-loop*)	4 fM 0.1 % *w*/w (pork/beef)	10 nM - 100 fM	This work

CRediT authorship contribution statement

Muhammad Ihda H.L. Zein: Writing – original draft, Software, Formal analysis. **Clianta Yudin Kharismasari:** Investigation, Formal analysis. **Ari Hardianto:** Writing – review & editing, Supervision, Software, Data curation. **Salma Nur Zakiyyah:** Visualization, Data curation. **Riezki Amalia:** Validation, Resources. **Mehmet Ozsoz:** Writing – review & editing, Supervision, Methodology. **Mara Mirasoli:** Writing – review & editing, Supervision. **Irkham:** Writing – review & editing, Visualization. **Yeni Wahyuni Hartati:** Writing – review & editing, Supervision, Funding acquisition, Conceptualization.

Declaration of competing interest

The authors declare no competing interests.

Acknowledgments

The research was funded by the Academic Leadership Grant Scheme No. 1655/UN6.3.1/PT.00/2024, provided by Universitas Padjadjaran.

Appendix A. Supplementary data

Supplementary data to this article can be found online at https://doi.org/10.1016/j.sbsr.2025.100755.

Data availability

Data will be made available on request.

References

[1] Y.W. Hartati, I. Irkham, I. Sumiati, S. Wyantuti, S. Gaffar, S.N. Zakiyyah, M.I.H. L. Zein, M. Ozsoz, The optimization of a label-free electrochemical DNA biosensor for detection of Sus scrofa mtDNA as food adulterations, Biosensors 13 (2023), https://doi.org/10.3390/bios13060657.
[2] T.J. Raharjo, A. Rohman, Analysis of pork contamination in Abon using mitochondrial D-Loop22 primers using real time polymerase chain reaction method, Int. Food Res. J. 23 (2016) 370–374.
[3] N.S. Karabasanavar, S.P. Singh, D. Kumar, S.N. Shebannavar, Detection of pork adulteration by highly-specific PCR assay of mitochondrial D-loop, Food Chem. 145 (2014) 530–534, https://doi.org/10.1016/j.foodchem.2013.08.084.
[4] Y. Erwanto, M. Zainal Abidin, E.Y.P. Muslim, A. Rohman Sugiyono, Identification of pork contamination in meatballs of Indonesia local market using polymerase chain reaction-restriction fragment length polymorphism (PCR-RFLP) analysis, Asian-Australasian, J. Anim. Sci. 27 (2014) 1487–1492, https://doi.org/10.5713/ajas.2014.14014.
[5] M.E. Ali, U. Hashim, S. Mustafa, Y.B. Che Man, T.S. Dhahi, M. Kashif, M.K. Uddin, S.B. Abd Hamid, Analysis of pork adulteration in commercial meatballs targeting porcine-specific mitochondrial cytochrome b gene by TaqMan probe real-time polymerase chain reaction, Meat Sci. 91 (2012) 454–459, https://doi.org/10.1016/j.meatsci.2012.02.031.
[6] M.E. Ali, M.A. Razzak, S.B.A. Hamid, M.M. Rahman, M. Al Amin, N.R.A. Rashid, Asing, Multiplex PCR assay for the detection of five meat species forbidden in Islamic foods, Food Chem. 177 (2015) 214–224, https://doi.org/10.1016/j.foodchem.2014.12.098.
[7] H.D. Nguyen, T.A. Bui, P.T. Nguyen, O.T.P. Kim, T.T.B. Vo, The complete mitochondrial genome sequence of the indigenous I pig (*Sus scrofa*) in Vietnam, Asian-Australasian, J. Anim. Sci. 30 (2016) 930–937, https://doi.org/10.5713/ajas.16.0608.
[8] A. Muflihah, P. Hardianto, S. Kusumaningtyas, Y.W. Prabowo, Hartati, DNA-based detection of pork content in food, Heliyon 9 (2023) e14418, https://doi.org/10.1016/j.heliyon.2023.e14418.
[9] R. Barrangou, L.A. Marraffini, CRISPR-Cas systems: prokaryotes upgrade to adaptive immunity, Mol. Cell 54 (2014) 234–244, https://doi.org/10.1016/j.molcel.2014.03.011.
[10] S.N. Zakiyyah, A.U. Ibrahim, M.S. Babiker, S. Gaffar, M. Ozsoz, M.I.H.L. Zein, Y. W. Hartati, Detection of tropical diseases caused by mosquitoes using CRISPR-based biosensors, Trop. Med. Infect. Dis. 7 (2022), https://doi.org/10.3390/tropicalmed7100309.
[11] Y. Dai, R.A. Somoza, L. Wang, J.F. Welter, Y. Li, A.I. Caplan, C.C. Liu, Exploring the trans-cleavage activity of CRISPR-Cas12a (cpf1) for the development of a universal electrochemical biosensor, Angew. Chem. 58 (2019) 17399–17405, https://doi.org/10.1002/anie.201910772.
[12] L. Curti, F. Pereyra-Bonnet, C.A. Gimenez, An ultrasensitive, rapid, and portable coronavirus SARS-CoV-2 sequence detection method based on CRISPR-Cas12, BioRxiv (2020), https://doi.org/10.1101/2020.02.29.971127v1.abstract, 2020.02.29.971127.
[13] Y. Wu, Y. Dong, Y. Shi, H. Yang, J. Zhang, M.R. Khan, S. Deng, G. He, Q. He, Y. Lv, R. Deng, CRISPR-Cas12-based rapid authentication of halal food, J. Agric. Food Chem. 69 (2021) 10321–10328, https://doi.org/10.1021/acs.jafc.1c03078.
[14] Y. Chen, X. Xu, J. Wang, Y. Zhang, W. Zeng, Y. Liu, X. Zhang, Photoactivatable CRISPR/Cas12a strategy for one-pot DETECTR molecular diagnosis, Anal. Chem. 94 (2022) 9724–9731, https://doi.org/10.1021/acs.analchem.2c01193.
[15] Z. Ali, R. Aman, A. Mahas, G.S. Rao, M. Tehseen, T. Marsic, R. Salunke, A. K. Subudhi, S.M. Hala, S.M. Hamdan, A. Pain, F.S. Alofi, A. Alsomali, A.M. Hashem, A. Khogeer, N.A.M. Almontashiri, M. Abedalthagafi, N. Hassan, M.M. Mahfouz, iSCAN: an RT-LAMP-coupled CRISPR-Cas12 module for rapid, sensitive detection of SARS-CoV-2, Virus Res. 288 (2020) 198129, https://doi.org/10.1016/j.virusres.2020.198129.
[16] C.L. Fasching, V. Servellita, B. McKay, V. Nagesh, J.P. Broughton, A. Sotomayor-Gonzalez, B. Wang, N. Brazer, K. Reyes, J. Streithorst, R.N. Deraney, E. Stanfield, C. G. Hendriks, B. Fung, S. Miller, J. Ching, J.S. Chen, C.Y. Chiu, COVID-19 variant detection with a high-Fidelity CRISPR-Cas12 enzyme, J. Clin. Microbiol. 60 (2022), https://doi.org/10.1128/jcm.00261-22.
[17] Y. Wang, X. Xia, M. Wu, Q. Sun, W. Zhang, Y. Qiu, R. Deng, A. Luo, Species-level monitoring of key Bacteria in fermentation processes using single-nucleotide resolved nucleic acid assays based on CRISPR/Cas12, J. Agric. Food Chem. 71 (2023) 13147–13155, https://doi.org/10.1021/acs.jafc.3c04775.
[18] N. Serrano, Ò. Castilla, C. Ariño, M. Diaz-Cruz, J. Díaz-Cruz, Commercial screen-printed electrodes based on carbon nanomaterials for a fast and cost-effective Voltammetric determination of paracetamol, ibuprofen and caffeine in water samples, Sensors 19 (2019) 4039, https://doi.org/10.3390/s19184039.
[19] T.-C. Chou, K.-Y. Wu, F.-X. Hsu, C.-K. Lee, Pt-MWCNT modified carbon electrode strip for rapid and quantitative detection of H 2 O 2 in food, J. Food Drug Anal. 26 (2018) 662–669, https://doi.org/10.1016/j.jfda.2017.08.005.
[20] S.N. Zakiyyah, N. Irkham, Y. Einaga, N.S. Gultom, R.P. Fauzia, G.T.M. Kadja, S. Gaffar, M. Ozsoz, Y.W. Hartati, Green synthesis of ceria nanoparticles from cassava tubers for electrochemical aptasensor detection of SARS-CoV-2 on a screen-printed carbon electrode, ACS Appl. Bio. Mater. 7 (2024) 2488–2498, https://doi.org/10.1021/acsabm.4c00088.
[21] T.F.H. Lestari, R. Setiyono, N. Tristina, Y. Sofiatin, Y.W. Hartati, The optimization of electrochemical immunosensors to detect epithelial sodium channel as a biomarker of hypertension, Admet DMPK (2023), https://doi.org/10.5599/admet.1629.
[22] M. Fajriyah, Y. Rohmatulloh, S. Gaffar, A. Angraeni, Y. Hartati, Electrochemical biosensor for mitochondrial DNA of *Sus Scrofa* detection using a cerium-modified screen printed carbon electrode, in: Proc. 1st Int. Conf. Islam. Sci. Technol. ICONISTECH 2019, 11–12 July 2019, EAI, Bandung, Indones, 2020, https://doi.org/10.4108/eai.11-7-2019.2297724.
[23] M.M. Ba-Abbad, P.V. Chai, M.S. Takriff, A. Benamor, A.W. Mohammad, Optimization of nickel oxide nanoparticle synthesis through the sol–gel method using Box–Behnken design, Mater. Des. 86 (2015) 948–956, https://doi.org/10.1016/j.matdes.2015.07.176.
[24] M.I.H.L. Zein, A. Hardianto, I. Irkham, Y.W. Hartati, Identification of CRISPR/Cas12a (Cpf1) guideRNA sequence targeting the mitochondrial DNA D-loop region in wild pig (Sus scrofa) through homology difference and mismatch analysis, Trends Sci. 21 (2024) 7603. https://tis.wu.ac.th/index.php/tis/article/view/7603.
[25] E.I. Fazrin, A.K. Sari, R. Setiyono, S. Gaffar, Y. Sofiatin, H.H. Bahti, Y.W. Hartati, The selectivity and stability of epithelial Sodium Channel (ENaC) aptamer as an electrochemical Aptasensor, Anal. Bioanal. Electrochem. 14 (2022) 715–729.

[26] C. Wu, Z. Chen, C. Li, Y. Hao, Y. Tang, Y. Yuan, L. Chai, T. Fan, J. Yu, X. Ma, O. A. Al-Hartomy, S. Wageh, A.G. Al-Sehemi, Z. Luo, Y. He, J. Li, Z. Xie, H. Zhang, CRISPR-Cas12a-empowered electrochemical biosensor for rapid and ultrasensitive detection of SARS-CoV-2 Delta variant, Nano-Micro Lett. 14 (2022) 159, https://doi.org/10.1007/s40820-022-00888-4.

[27] T.D. Golden, A.Q. Wang, Anodic electrodeposition of cerium oxide thin films, J. Electrochem. Soc. 150 (2003) C621, https://doi.org/10.1149/1.1596165.

[28] A.K. Sari, Y.W. Hartati, S. Gaffar, I. Anshori, D. Hidayat, H.L. Wiraswati, The optimization of an electrochemical aptasensor to detect RBD protein S SARS-CoV-2 as a biomarker of COVID-19 using screen-printed carbon electrode/AuNP, J. Electrochem. Sci. Eng. 12 (2022) 219–235, https://doi.org/10.5599/jese.1206.

[29] E. Barou, M. Bouvet, O. Heintz, R. Meunier-Prest, Electrochemistry of methylene blue at an alkanethiol modified electrode, Electrochim. Acta 75 (2012) 387–392, https://doi.org/10.1016/j.electacta.2012.05.017.

[30] R.S. Syafira, M.J. Devi, S. Gaffar, I. Irkham, W. Kurnia, Y. Arnafia, N. Einaga, A. R. Syakir, Y.W. Hartati Noviyanti, Hydroxyapatite-gold modified screen-printed carbon electrode for selective SARS-CoV-2 antibody Immunosensor, ACS Appl. Bio. Mater. 7 (2024) 950–960, https://doi.org/10.1021/acsabm.3c00953.

[31] Q. Zhao, Q. Wu, P. Ma, L. Xu, F. Zhang, D. Li, X. Liu, S. Xu, Y. Sun, D. Song, X. Wang, Selective and sensitive fluorescence detection method for pig IgG based on competitive immunosensing strategy and magnetic bioseparation, Talanta 195 (2019) 103–108, https://doi.org/10.1016/j.talanta.2018.11.041.

[32] Q. Wu, Y. Sun, P. Ma, D. Zhang, S. Li, X. Wang, D. Song, Gold nanostar-enhanced surface plasmon resonance biosensor based on carboxyl-functionalized graphene oxide, Anal. Chim. Acta 913 (2016) 137–144, https://doi.org/10.1016/j.aca.2016.01.063.

[33] S.A. Lim, M.U. Ahmed, A label free electrochemical immunosensor for sensitive detection of porcine serum albumin as a marker for pork adulteration in raw meat, Food Chem. 206 (2016) 197–203, https://doi.org/10.1016/j.foodchem.2016.03.063.

[34] J.M.R. Flauzino, E.P. Nguyen, Q. Yang, G. Rosati, D. Panáček, A.G. Brito-Madurro, J.M. Madurro, A. Bakandritsos, M. Otyepka, A. Merkoçi, Label-free and reagentless electrochemical genosensor based on graphene acid for meat adulteration detection, Biosens. Bioelectron. 195 (2022), https://doi.org/10.1016/j.bios.2021.113628.